

Pair density waves in spinless media

Marios Georgiou^{1,2} and Georgios Varelogiannis¹

¹*Department of Physics, National Technical University of Athens, GR-15780 Athens, Greece*

²*Department of Physics, Loughborough University, Loughborough LE11 3TU, United Kingdom*



(Received 29 July 2018; revised 21 July 2020; accepted 24 August 2020; published 15 September 2020)

We study the competition of homogeneous SC with pair density wave states in a spinless formalism focusing on systems with band structures that exhibit commensurate nesting features. We show that a specific triplet commensurate pair density wave superconducting (SC) state, the staggered d -wave triplet state (triplet dPDW), may coexist with homogeneous triplet SC states and even dominate, eliminating them for small deviations from nesting. We point out qualitative characteristics of the tunneling density of states and specific heat that identify this triplet dPDW state. Our results are qualitatively extendable to similar systems with nested band structures.

DOI: [10.1103/PhysRevB.102.094514](https://doi.org/10.1103/PhysRevB.102.094514)

I. INTRODUCTION

Singlet superconductivity (SC) and ferromagnetism (FM) are directly competing phenomena. The discovery of SC coexisting with FM in UGe_2 [1] and other bulk FM-SC [2,3] in heterostructures where the proximity of SC and FM is enforced [4–6] necessarily involves exotic spin-triplet SC states. Numerous theoretical models with homogeneous triplet SC states that are possibly odd in frequency have been proposed [7–11]. For the two-dimensional SC state that develops at the interfaces of some oxide insulators like $LaAlO_3/SrTiO_3$ [12] in the presence of FM [13] a modulated or pair density wave (PDW) triplet state of Fulde-Ferrell-Larkin-Ovchinnikov (FFLO) type has also been suggested [14]. The observation of proximity-induced SC in the half-metallic (fully polarized) FM CrO_2 in contact with SC $NbTiN$ [4] demonstrates that effectively spinless systems may exhibit SC as well.

In the present work, we address the question of competition of homogeneous SC with pair density wave states in a fully spin polarized medium, using a band dispersion with *commensurate nesting vector* \mathbf{Q} to accommodate the pair density wave states. The competition of all SC condensates allowed by symmetry is studied systematically, and we show that a triplet SC state exhibiting commensurate density wave modulation of the superfluid density may coexist with, or even dominate and eliminate, the homogeneous (zero momentum) triplet SC for small deviations from nesting. When this triplet commensurate pair density wave SC (*triplet PDW*) state dominates, we have robust *gapless* SC. We report phase transitions between the various types of accessible triplet SC states, including transitions between *gapped* and *gapless* SC states, as well as qualitative physical characteristics in the density of states and specific heat that would allow us to identify the type of triplet SC in which the system of interest is. In this work $\mathbf{Q} = (\pi, \pi)$; however, our results are qualitatively extendable to similar systems with nesting properties at different wave vectors with the appropriate changes to the PDW's wave vector.

A similar triplet PDW state channel has been suggested to occur in the high-field SC state of $CeCoIn_5$ coexisting with singlet SC and spin density waves [15,16], explaining fascinating neutron scattering results [17]. There have also been studies of PDW in the singlet channel, also called η pairing [18–24], mainly motivated by the extraordinary physics in the pseudogap and other stripe regimes of cuprates [25,26].

II. MODEL, SYMMETRIES, AND PHASE COMPETITION

Our starting point is a BCS-type Hamiltonian with frozen spin:

$$\mathcal{H} = \sum_{\mathbf{k}} \xi_{\mathbf{k}} c_{\mathbf{k}}^{\dagger} c_{\mathbf{k}} - \sum_{\mathbf{k}} (\Delta_{\mathbf{k}} c_{\mathbf{k}}^{\dagger} c_{-\mathbf{k}}^{\dagger} + \text{H.c.}) - \sum_{\mathbf{k}} (\Pi_{\mathbf{k}} c_{\mathbf{k}}^{\dagger} c_{-(\mathbf{k}+\mathbf{Q})}^{\dagger} + \text{H.c.}). \quad (1)$$

The first term describes a tight-binding dispersion which generically can be written as the sum of particle-hole-symmetric terms and particle-hole-asymmetric terms: $\xi_{\mathbf{k}} = \gamma_{\mathbf{k}} + \delta_{\mathbf{k}} - \mu$. When $\delta_{\mathbf{k}} = 0$, there is particle-hole symmetry or perfect nesting, while finite values of $\delta_{\mathbf{k}}$ destroy the nesting conditions. The second term, $\Delta_{\mathbf{k}} = \sum_{\mathbf{k}'} V_{\mathbf{k},\mathbf{k}'}^{\Delta} \langle c_{-\mathbf{k}'} c_{\mathbf{k}'} \rangle$, represents unconventional SC with zero pair momentum, and the last term, $\Pi_{\mathbf{k}} = \sum_{\mathbf{k}'} V_{\mathbf{k},\mathbf{k}'}^{\Pi} \langle c_{-(\mathbf{k}+\mathbf{Q})} c_{\mathbf{k}'} \rangle$, is the triplet PDW or modulated SC state. Although our PDW bears some resemblance to the FFLO state [27] because Cooper pairs have finite total pair momentum and the superfluid density is inhomogeneous, they are fundamentally different. In fact, our PDW is a spin-triplet state, whereas the FFLO is a spin singlet trying to survive the Zeeman field. The wave vector of the superfluid modulation in our triplet PDW is the commensurate nesting vector \mathbf{Q} . In the FFLO state instead, the wave vector of the superfluid modulation is variable, scaling with the magnitude of the magnetic field.

The effective interactions of the itinerant quasiparticles $V_{\mathbf{k},\mathbf{k}'}^{\Delta}$, $V_{\mathbf{k},\mathbf{k}'}^{\Pi}$ may have a purely electronic origin in the case of FM superconductors. However, our approach is generic

irrespective of the microscopic origin of the effective interactions, and the validity of our findings is generic as well. In the case of heterostructures, we assume within our approach that the effective potentials incorporate the proximity effects as well. Naturally, we would expect in that case a real-space dependence of the potentials, which we neglect here. We focus on only qualitative symmetry questions that would not be affected by a smooth space dependence. In fact, the modulation of the superfluid density in our triplet PDW state has a wavelength that is negligible compared to the coherence length and the characteristic lengths of the heterostructure. We therefore expect our qualitative findings to hold for bulk materials and for nanostructures as well.

To treat both types of SC order parameters (OPs) in a compact manner we introduce a Nambu-type representation using the spinor $\Psi_{\mathbf{k}}^{\dagger} = (c_{\mathbf{k}}^{\dagger}, c_{-\mathbf{k}}, c_{\mathbf{k}+\mathbf{Q}}^{\dagger}, c_{-\mathbf{k}-\mathbf{Q}})$, and we use the basis provided by the tensor products $\hat{\rho}_i \otimes \hat{\tau}_i$, where $\hat{\rho}_i, \hat{\tau}_i$ are the usual 2×2 Pauli matrices. The absence of spin index in the Hamiltonian affects the symmetry classification of the acceptable *triplet* SC states, for which we produced a systematic phase map. In fact, the OPs are normally classified by their behavior under inversion (\hat{I}) $\mathbf{k} \rightarrow -\mathbf{k}$, translation ($\hat{t}_{\mathbf{Q}}$), $\mathbf{k} \rightarrow \mathbf{k} + \mathbf{Q}$ and time reversal (\hat{T}).

Instead of the latter we may use complex conjugation \hat{K} which is related to time reversal via the relations $\hat{T} \equiv \hat{I}\hat{K}(\Delta/\Pi)$. Since the spins are frozen, the homogeneous ($\mathbf{q} = 0$) SC pair states may have only odd parity: $\Delta_{-\mathbf{k}} = -\Delta_{\mathbf{k}}$. Under translation we have both signs, $\Delta_{\mathbf{k}+\mathbf{Q}} = \pm\Delta_{\mathbf{k}}$, and under \hat{T} we get $\hat{T}\Delta_{\mathbf{k}} = -\Delta_{\mathbf{k}}^*$. Triplet PDW states may have both parities, $\Pi_{-\mathbf{k}} = \pm\Pi_{\mathbf{k}}$, and both signs under translation since $\Pi_{\mathbf{k}+\mathbf{Q}} = -\Pi_{-\mathbf{k}} = \mp\Pi_{\mathbf{k}}$. Classifying the SC states with respect to \hat{K}, \hat{I} , and $\hat{t}_{\mathbf{Q}}$ we have four homogeneous states: $\Delta_{\mathbf{k}}^{R--}, \Delta_{\mathbf{k}}^{R+-}, \Delta_{\mathbf{k}}^{I--},$ and $\Delta_{\mathbf{k}}^{I+-}$ and four PDW states: $\Pi_{\mathbf{k}}^{R+-}, \Pi_{\mathbf{k}}^{R++}, \Pi_{\mathbf{k}}^{I+-},$ and $\Pi_{\mathbf{k}}^{I++}$. Here the first index R or I indicates whether the OP is real or imaginary, the second index \pm indicates parity under inversion \hat{I} , and the last index denotes gap symmetry under $\hat{t}_{\mathbf{Q}}$. The symmetry properties of the OPs under inversion \hat{I} and translation $\hat{t}_{\mathbf{Q}}$ imply a specific structure in \mathbf{k} space. Every OP $M_{\mathbf{k}}$ is written in the form $M_{\mathbf{k}} = M f_{\mathbf{k}}$, where the *form factors* $f_{\mathbf{k}}$ belong to the different irreducible representations of the point group.

According to the above symmetry classification there exist 16 possible pairs of competing homogeneous and modulated SC states. Using our formalism, we calculate Green's functions and, from them, self-consistent systems of coupled gap equations for each case, ending up with two different sets of coupled gap equations. Specifically, the pairs

$$\begin{aligned} \Delta_{\mathbf{k}}^{R--} & \text{ with } \Pi_{\mathbf{k}}^{R++}, & \Delta_{\mathbf{k}}^{I--} & \text{ with } \Pi_{\mathbf{k}}^{I+-}, \\ \Delta_{\mathbf{k}}^{R+-} & \text{ with } \Pi_{\mathbf{k}}^{I+-}, & \Delta_{\mathbf{k}}^{I+-} & \text{ with } \Pi_{\mathbf{k}}^{R+-}, \\ \Delta_{\mathbf{k}}^{R--} & \text{ with } \Pi_{\mathbf{k}}^{I+-}, & \Delta_{\mathbf{k}}^{I--} & \text{ with } \Pi_{\mathbf{k}}^{R++}, \\ \Delta_{\mathbf{k}}^{R+-} & \text{ with } \Pi_{\mathbf{k}}^{R+-}, & \Delta_{\mathbf{k}}^{I+-} & \text{ with } \Pi_{\mathbf{k}}^{I+-} \end{aligned} \quad (2)$$

obey the type I equations, which are

$$\Delta_{\mathbf{k}} = \sum_{\mathbf{k}'} V_{\mathbf{k},\mathbf{k}'}^{\Delta} \Delta_{\mathbf{k}'} \sum_{\pm} \frac{1}{4E_{\pm}(\mathbf{k}')} \tanh\left(\frac{E_{\pm}(\mathbf{k}')}{2T}\right),$$

$$\begin{aligned} \Pi_{\mathbf{k}} &= \sum_{\mathbf{k}'} V_{\mathbf{k},\mathbf{k}'}^{\Pi} \Pi_{\mathbf{k}'} \sum_{\pm} \frac{\sqrt{(\delta_{\mathbf{k}'} - \mu)^2 + \Pi_{\mathbf{k}'}^2} \pm \gamma_{\mathbf{k}'}}{4E_{\pm}(\mathbf{k}')\sqrt{(\delta_{\mathbf{k}'} - \mu)^2 + \Pi_{\mathbf{k}'}^2}} \\ &\times \tanh\left(\frac{E_{\pm}(\mathbf{k}')}{2T}\right), \end{aligned} \quad (3)$$

where the dispersion relations are given by

$$E_{\pm}(\mathbf{k}) = \sqrt{\left[\sqrt{(\delta_{\mathbf{k}} - \mu)^2 + \Pi_{\mathbf{k}}^2} \pm \gamma_{\mathbf{k}}\right]^2 + \Delta_{\mathbf{k}}^2}. \quad (4)$$

Notice that the competing pairs in the left and right columns in (2) have identical behavior under \hat{I} and $\hat{t}_{\mathbf{Q}}$; that is, they are represented by the same form factors. Furthermore, they obey the same self-consistent equations given by (3). Thus, the solutions of the coupled gap equations coincide, and we need to numerically study only half of the eight competing pairs. We solved numerically the type I equations (3) for the pairs

$$\begin{aligned} \Delta_{\mathbf{k}}^{I--} & \text{ with } \Pi_{\mathbf{k}}^{I+-}, & \Delta_{\mathbf{k}}^{I+-} & \text{ with } \Pi_{\mathbf{k}}^{R++}, \\ \Delta_{\mathbf{k}}^{I--} & \text{ with } \Pi_{\mathbf{k}}^{R+-}, & \Delta_{\mathbf{k}}^{I+-} & \text{ with } \Pi_{\mathbf{k}}^{I+-}. \end{aligned} \quad (5)$$

The remaining eight pairs,

$$\begin{aligned} \Delta_{\mathbf{k}}^{R--} & \text{ with } \Pi_{\mathbf{k}}^{R+-}, & \Delta_{\mathbf{k}}^{I--} & \text{ with } \Pi_{\mathbf{k}}^{I+-}, \\ \Delta_{\mathbf{k}}^{R+-} & \text{ with } \Pi_{\mathbf{k}}^{I+-}, & \Delta_{\mathbf{k}}^{I+-} & \text{ with } \Pi_{\mathbf{k}}^{R+-}, \\ \Delta_{\mathbf{k}}^{R--} & \text{ with } \Pi_{\mathbf{k}}^{I+-}, & \Delta_{\mathbf{k}}^{I--} & \text{ with } \Pi_{\mathbf{k}}^{R++}, \\ \Delta_{\mathbf{k}}^{R+-} & \text{ with } \Pi_{\mathbf{k}}^{R+-}, & \Delta_{\mathbf{k}}^{I+-} & \text{ with } \Pi_{\mathbf{k}}^{I+-}, \end{aligned} \quad (6)$$

obey the type II equations, which in turn are

$$\begin{aligned} \Delta_{\mathbf{k}} &= \sum_{\mathbf{k}'} V_{\mathbf{k},\mathbf{k}'}^{\Delta} \Delta_{\mathbf{k}'} \sum_{\pm} \frac{B_{\mathbf{k}'} \pm \Pi_{\mathbf{k}'}^2}{4E_{\pm}(\mathbf{k}')B_{\mathbf{k}'}} \tanh\left(\frac{E_{\pm}(\mathbf{k}')}{2T}\right), \\ \Pi_{\mathbf{k}} &= \sum_{\mathbf{k}'} V_{\mathbf{k},\mathbf{k}'}^{\Pi} \Pi_{\mathbf{k}'} \sum_{\pm} \frac{B_{\mathbf{k}'} \pm \gamma_{\mathbf{k}'}^2 \pm \Delta_{\mathbf{k}'}^2}{4E_{\pm}(\mathbf{k}')B_{\mathbf{k}'}} \tanh\left(\frac{E_{\pm}(\mathbf{k}')}{2T}\right), \end{aligned} \quad (7)$$

where $B_{\mathbf{k}}$ and $E_{\pm}(\mathbf{k})$ are given by

$$\begin{aligned} B_{\mathbf{k}} &= \sqrt{\gamma_{\mathbf{k}}^2 [(\delta_{\mathbf{k}} - \mu)^2 + \Pi_{\mathbf{k}}^2] + \Delta_{\mathbf{k}}^2 \Pi_{\mathbf{k}}^2}, \\ E_{\pm}(\mathbf{k}) &= \sqrt{\gamma_{\mathbf{k}}^2 + (\delta_{\mathbf{k}} - \mu)^2 + \Delta_{\mathbf{k}}^2 + \Pi_{\mathbf{k}}^2 \pm 2B_{\mathbf{k}}}. \end{aligned} \quad (8)$$

In this case too we notice that the competing pairs in the left column in (6) have behavior under \hat{I} and $\hat{t}_{\mathbf{Q}}$ identical to that of the competing pairs in the right column. Therefore, we need to numerically study only half of the competing pairs. We studied the following type II pairs:

$$\begin{aligned} \Delta_{\mathbf{k}}^{I--} & \text{ with } \Pi_{\mathbf{k}}^{I+-}, & \Delta_{\mathbf{k}}^{I+-} & \text{ with } \Pi_{\mathbf{k}}^{R+-}, \\ \Delta_{\mathbf{k}}^{I--} & \text{ with } \Pi_{\mathbf{k}}^{R+-}, & \Delta_{\mathbf{k}}^{I+-} & \text{ with } \Pi_{\mathbf{k}}^{I+-}. \end{aligned} \quad (9)$$

The effective potentials $V_{\mathbf{k},\mathbf{k}'}^{\Delta}, V_{\mathbf{k},\mathbf{k}'}^{\Pi}$ have the form $V_{\mathbf{k},\mathbf{k}'} = V f_{\mathbf{k}} f_{\mathbf{k}'}$ (separable potentials). We have solved self-consistently the above systems of equations on a square lattice with $\gamma_{\mathbf{k}} = -t_1(\cos k_x + \cos k_y)$, $\delta_{\mathbf{k}} = -t_2 \cos k_x \cos k_y$, $\mu = 0$, and $\mathbf{Q} = (\pi, \pi)$. The choice of a *tetragonal* dispersion is motivated, in part, by the fact that half-metallic systems such as CrO_2 exhibit a tetragonal structure; however, our qualitative findings are generic. The corresponding

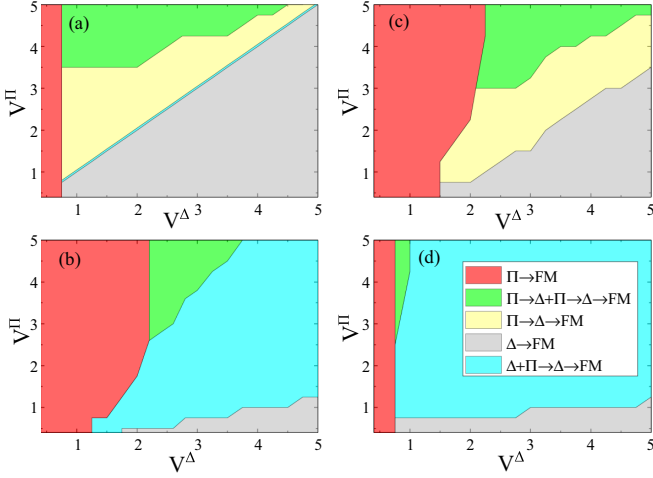


FIG. 1. Maps of the dependence of phase sequences on the effective interactions V^Δ and V^Π for low temperature. The colors indicate the different cascades of phases obtained when t_2/t_1 grows starting from zero ($\mu = 0$ everywhere). All phases coexist with ferromagnetism (FM). The phase indicated as FM is only ferromagnetic; no SC gap is finite. The couple of (a) Π^{I+-} with Δ^{I--} , (b) Π^{I+-} with Δ^{I-+} , (c) Π^{R+-} with Δ^{I-+} , and (d) Π^{R+-} with Δ^{I--} . The potentials are in units of t_1 .

form factors belong to irreducible representations of the tetragonal group D_{4h} . Specifically, $\Delta_{\mathbf{k}}^{I--} \sim \sin k_x + \sin k_y$ (s wave), $\Delta_{\mathbf{k}}^{I-+}, \Pi_{\mathbf{k}}^{I-+} \sim \sin(k_x + k_y)$ (p wave), and $\Pi_{\mathbf{k}}^{R+-} \sim \cos k_x - \cos k_y$ (d wave). For every competing pair we have performed a large number of self-consistent calculations varying pairing potentials in the two channels, temperatures, and ratios t_2/t_1 .

The first important result is that the triplet PDW $\Pi_{\mathbf{k}}^{QI+-}$ OP can never survive. Specifically, the $\Pi_{\mathbf{k}}^{QI+-}$ gap is zero regardless of the values of the pairing potentials and the particle-hole asymmetry t_2/t_1 term. We conclude that although the state $\Pi_{\mathbf{k}}^{QI+-}$ is allowed by symmetry, it is never realized. Therefore, we report only results about the relevant competition of the remaining $\Pi_{\mathbf{k}}^{R+-}$ and $\Pi_{\mathbf{k}}^{I+-}$ [triplet d -wave PDW (dPDW)] with both zero-momentum SC states.

The phase sequences as t_2/t_1 grows starting from zero and for various values of the pairing potentials for the competition of $\Pi_{\mathbf{k}}^{I+-}$ ($\Pi_{\mathbf{k}}^{R+-}$) with $\Delta_{\mathbf{k}}^{I--}$ or $\Delta_{\mathbf{k}}^{I-+}$ are shown in the respective panels of Fig. 1. Colors in Fig. 1 indicate different cascades of phases observed when the ratio t_2/t_1 grows starting from zero in each region of the map. The variation of t_2/t_1 may simulate various effects such as chemical doping or stress effects as well as proximity effects. Since we consider a spin-polarized background, all states coexist with FM, and the transitions to the FM state reported at high values of t_2/t_1 have the meaning of a transition to a state that is only ferromagnetic with no SC OPs present.

It is obvious that the competition of Π^{I+-} with the two homogeneous SC states [Figs. 1(a) and 1(b)] has the same qualitative features as the competition of Π^{R+-} [Figs. 1(c) and 1(d)], namely, the same cascades of phases as t_2/t_1 grows (indicated by regions in different colors) appear. Furthermore,

all cases share the characteristic feature that the triplet dPDW state is finite in the largest part of the maps of the pairing potentials. Thus, since we do not limit ourselves to a specific microscopic model that could correspond to a specific value for the pairing potentials, the existence of the triplet dPDW phase can be considered generically plausible. In the following we focus on the competition of $\Pi_{\mathbf{k}}^{R+-}$ with the two Δ states.

The interplay of $\Pi_{\mathbf{k}}^{R+-}$ with $\Delta_{\mathbf{k}}^{I--}$ favors the coexistence of both ($\mathbf{q} = \mathbf{0}$ and $\mathbf{q} = \mathbf{Q}$) SC states at low T over a wide range of values of the pairing potentials [Fig. 1(d)]. The transition from a coexistence state to a homogeneous ($\mathbf{q} = \mathbf{0}$) SC state as t_2/t_1 grows is always continuous (*second order*) and dominates the V^Δ, V^Π parameter space.

The low-temperature regime is different in the interplay of $\Pi_{\mathbf{k}}^{R+-}$ with $\Delta_{\mathbf{k}}^{I-+}$. The coexistence of the two SC states is allowed again but now is restricted to a small portion of the V^Δ, V^Π map [Fig. 1(c)]. The most interesting feature now is the domination of the triplet dPDW (modulated SC) state for the smaller values of t_2/t_1 . Thus, in this case the formation of the Π^{R+-} triplet dPDW state is favored. As particle-hole asymmetry grows (t_2/t_1 grows), we may have transitions from a triplet dPDW to a state of coexistence or to a homogeneous SC state.

We note that in the case of both Δ and Π being nonzero, a charge density wave (CDW) is generated. This can be seen by diagonalizing the corresponding mean-field Hamiltonian using a Bogolyubov transformation and calculating the ground state expectation value $\langle c_{\mathbf{k}}^\dagger c_{\mathbf{k}+\mathbf{Q}} \rangle$, which turns out to be finite. Specifically, for the coexistence of $\Delta_{\mathbf{k}}^{I--}$ with $\Pi_{\mathbf{k}}^{R+-}$ we have that $\langle c_{\mathbf{k}}^\dagger c_{\mathbf{k}+\mathbf{Q}} \rangle \sim i\Delta_{\mathbf{k}}$, i.e., an s -wave CDW. This CDW generation by a mixed state of a homogeneous SC and a PDW was also reported by Seo *et al.* in their work on cuprates [23]. Nevertheless, the appearance of the CDW order does not change the qualitative characteristics of the $\Delta + \Pi$ coexistence phase such as the specific heat and density of states (DOS) at low temperature, which we present later, since the Fermi surface consists of isolated Fermi points in both cases. However, when only the triplet dPDW state is present, no CDW order is generated since the expectation value $\langle c_{\mathbf{k}}^\dagger c_{\mathbf{k}+\mathbf{Q}} \rangle$ is zero. This shows that the triplet dPDW state indeed exists as a pure state.

A. Δ^{I-+} with Π^{R+-}

We show in Fig. 2 the dependence of the Δ^{I-+} and Π^{R+-} on t_2/t_1 at low T [Fig. 2(a)] and the phase diagram [Fig. 2(c)] obtained by the coupled-gap equations for $V^\Delta = V^\Pi = 0.75t_1$. Only the Π gap is finite at low temperature, in agreement with Fig. 1(c) for the specific values of V^Δ, V^Π . We stress that the Π gap not only is finite for $t_2/t_1 = 0$ but survives up to $t_2/t_1 = 0.115$. The critical temperature satisfies $T_c/t_1 = 0.045$. Introducing $\mu = 0.1$ to the above system results in the extension of the Π gap to higher t_2/t_1 values at low T . Indeed, the Π gap survives up to $t_2/t_1 = 0.212$, while the Δ gap remains zero [Fig. 2(b)]. In general, finite μ values favor the triplet dPDW state but none of the homogeneous $\Delta_{\mathbf{k}}^{I--}, \Delta_{\mathbf{k}}^{I-+}$ states. The critical temperature is maximum for $t_2/t_1 = 0.1$ and satisfies $T_c/t_1 = 0.045$ [Fig. 2(d)].

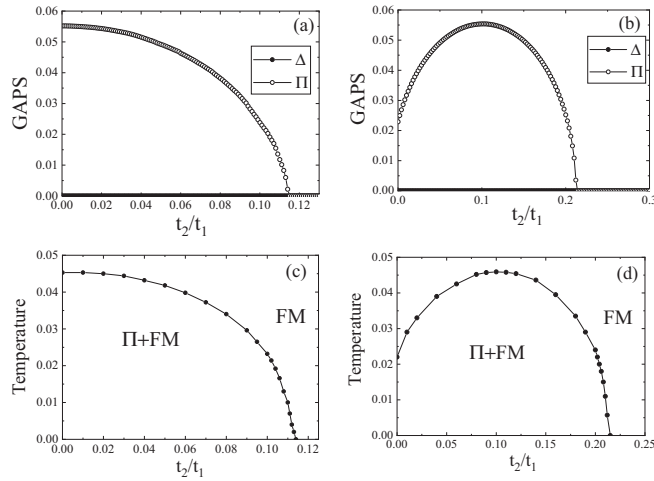


FIG. 2. Dependence of homogeneous $\Delta_{\mathbf{k}}^{I-+}$ and modulated $\Pi_{\mathbf{k}}^{R+-}$ SC gaps on t_2/t_1 at low T for (a) $\mu = 0$ and (b) $\mu = 0.1$. The Π gap is finite up to $t_2/t_1 = 0.115$ and $t_2/t_1 = 0.212$, respectively. (c) and (d) t_2/t_1 -temperature phase diagram for $\mu = 0$ and $\mu = 0.1$, respectively. Solid symbols mark second-order transitions. The values of the pairing potentials are $V^\Delta = V^\Pi = 0.75t_1$.

At low temperature the Π gap remains finite for higher t_2/t_1 values as the pairing potential V^Π increases. This is illustrated in Fig. 3, where we show the Π gap with respect to t_2/t_1 at low T for $V^\Delta = V^\Pi = 0.8t_1, t_1$, and $1.2t_1$ and $\mu = 0$. All three pairs of V^Δ, V^Π correspond to the $\Pi \rightarrow$ FM transition of Fig. 1(c); therefore, the Δ gap is zero with respect to t_2/t_1 in all three cases. As V^Π increases from $0.8t_1$ to t_1 , Π extends to $t_2/t_1 = 0.26$, while for $V^\Pi = 1.2$ it survives up to $t_2/t_1 = 0.4$.

However, as V^Π increases, the ratio T_c/t_1 also increases; that is, for $V^\Delta = V^\Pi = t_1$, $T_c/t_1 = 0.105$, while for $V^\Delta = V^\Pi = 1.2t_1$, $T_c/t_1 = 0.16$. It is straightforward that high values of the pairing potentials may lead, depending on the value of t_1 , to unrealistically high critical temperatures. We note that our study is not related to a specific material for which the value of t_1 has been determined by *ab initio* calculations. Therefore, our discussion will be limited to low V^Π values, i.e., $V^\Pi \lesssim t_1$. The same restriction applies also to the pairing potential of the $\Delta_{\mathbf{k}}^{I-+}$ state, whereas for the $\Delta_{\mathbf{k}}^{I--}$ state the

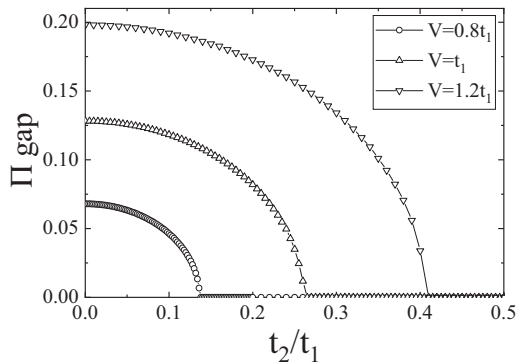


FIG. 3. Dependence of the $\Pi_{\mathbf{k}}^{R+-}$ gap on t_2/t_1 at low T . The values of the pairing potentials are $V^\Delta = V^\Pi = 0.8t_1, t_1$, and $1.2t_1$ and $\mu = 0$. The Δ gap is zero for all four pairs of the pairing potentials.

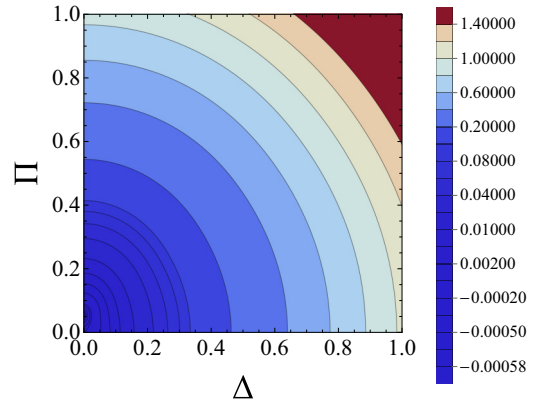


FIG. 4. Contour plot of the condensation free energy ΔF as a function of the OPs $\Pi_{\mathbf{k}}^{R+-}$ and $\Delta_{\mathbf{k}}^{I-+}$ at low T for $t_2/t_1 = 0$, $\mu = 0$, and $V^\Delta = V^\Pi = 0.75t_1$. The lowest value of ΔF is situated at the point $(\Delta, \Pi) = (0, 0.055t_1)$, which corresponds to the solutions of the respective coupled gap equations.

corresponding pairing potential should be $V^\Delta \lesssim 2t_1$ in order to have $T_c/t_1 \sim O(10^{-2})$. In the largest part of this parameter range of pairing potential values the triplet dPDW state dominates or coexists with zero-momentum SC states for small deviations from nesting.

The stability of the solutions of the self-consistent equations has been verified by free-energy calculations as well. The free-energy difference ΔF between the normal and condensed states is given by $\Delta F = \frac{\Delta^2}{V^\Delta} + \frac{\Pi^2}{V^\Pi} - \frac{1}{2\beta} \sum_{\mathbf{k}} \sum_{j=\pm, i=\pm} \ln\left(\frac{1+e^{-j\beta E_{\pm}(\mathbf{k})}}{1+e^{-j\beta \epsilon_{\pm}(\mathbf{k})}}\right)$, where $E_{\pm}(\mathbf{k})$ are the energy dispersions for each competing pair and $\epsilon_{\pm}(\mathbf{k})$ are the energy dispersions obtained when both gaps are zero. The safest way to ensure that the solutions of the coupled gap equations correspond to the minimum of the free-energy difference is to vary ΔF with respect to the magnitudes of the gaps and verify that ΔF attains its minimum for these values. We report in Fig. 4 the variations of the free-energy difference with $\Delta_{\mathbf{k}}^{I-+}$ and $\Pi_{\mathbf{k}}^{R+-}$ at low T for $t_2/t_1 = 0$, $\mu = 0$, and $V^\Delta = V^\Pi = 0.75t_1$. The solutions of the coupled gap equations in this case are $(\Delta, \Pi) = (0, 0.055t_1)$, i.e., dominance of the triplet dPDW state. It is clear that ΔF attains its minimum value for $(\Delta, \Pi) = (0, 0.055t_1)$; thus, the ground state consists solely of the triplet dPDW phase.

B. $\Delta_{\mathbf{k}}^{I--}$ with $\Pi_{\mathbf{k}}^{R+-}$

We show in Fig. 5 the dependence of $\Delta_{\mathbf{k}}^{I--}$ and $\Pi_{\mathbf{k}}^{R+-}$ on t_2/t_1 at low T [Fig. 5(a)] and their evolution with temperature [Fig. 5(b)] for $t_2/t_1 = 0$. The values of the pairing potentials are $V^\Delta = V^\Pi = 0.75t_1$ and correspond to the transition $\Pi + \Delta \rightarrow \Delta \rightarrow$ FM in Fig. 1(d) and $\mu = 0$. We stress that at low T for $t_2/t_1 = 0$ the values of the gaps are in full agreement with the ΔF minimum requirement, i.e., $(\Delta, \Pi) = (0.054t_1, 0.054t_1)$. As particle-hole asymmetry grows, the Π gap drops and becomes zero for $t_2/t_1 = 0.11$, while $\Delta_{\mathbf{k}}^{I--}$ survives up to high t_2/t_1 values. The t_2/t_1 transition from the coexistence phase to the homogeneous SC state is continuous. Both gaps have the same critical temperature, which satisfies $T_c/t_1 = 0.045$. We note that for $\mu = 0.1$ the Π gap extends up to $t_2/t_1 = 0.215$ at low T .

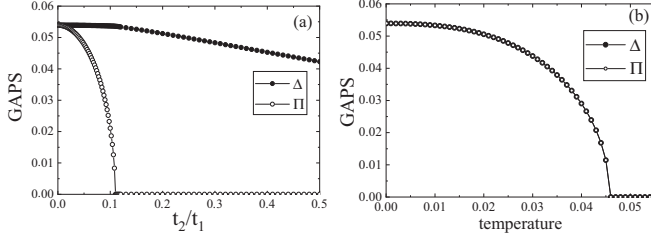


FIG. 5. Dependence of homogeneous Δ_k^{I--} and modulated Π_k^{R+-} SC gaps on (a) t_2/t_1 at low T , and (b) on temperature for $t_2/t_1 = 0$. The Δ_k^{I--} gap survives up to high t_2/t_1 values at low T . The values of the pairing potentials are $V^\Delta = V^\Pi = 0.75t_1$, and $\mu = 0$.

III. POSSIBLE EXPERIMENTAL IDENTIFICATION of Π_k^{R+-}

A question that naturally arises is how the exotic triplet dPDW state Π_k^{R+-} can be identified experimentally. Our analysis suggests that specific heat measurements at low T may be sufficient. Specifically, triplet dPDW states exhibit an extended Fermi surface (FS; line nodes) regardless of the value of the particle-hole asymmetry term, whereas both Δ states and the coexistence phase $\Delta + \Pi$ have isolated Fermi points. We note that the extended FS is also a feature of the spin-singlet η pairing [19]. Consequently, the triplet dPDW state Π_k^{R+-} is the sole SC state that exhibits a linear low- T behavior of the specific heat, and this is robust since it holds even for finite values of t_2/t_1 .

This is illustrated in Fig. 6, where the Fermi surface and the specific heat in the triplet dPDW phase (red) and in the homogeneous SC phase (blue) for $t_2/t_1 = 0.1$ are reported. We observe that in the Π_k^{R+-} phase the Fermi surface is extended, imposing the linear behavior of the specific heat at low T . On the other hand, in the Δ_k^{I--} phase we have only two Fermi points, and the specific heat at low T exhibits a polynomial behavior. This is also the case for the other homogeneous SC state Δ_k^{I--} as well as for the coexistence phase $\Delta + \Pi$. We stress that the specific heat exhibits the same low- T behavior

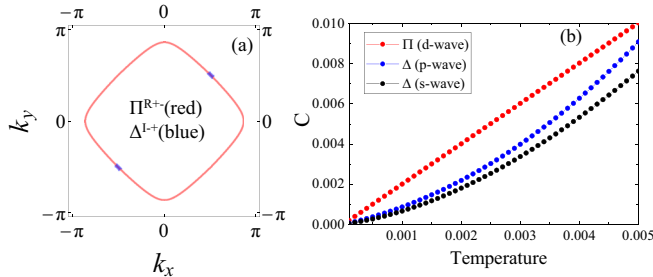


FIG. 6. (a) Fermi surface and (b) specific heat at low T in the Π_k^{R+-} state for $t_2/t_1 = 0.1$ and the Δ_k^{I--} state for $t_2/t_1 = 0.1$. The pairing potentials are $V^\Delta = 1.8t_1$ and $V^\Pi = 0.75t_1$, and $\mu = 0$. The extended FS in the triplet dPDW state causes the linear behavior of the specific heat, whereas the polynomial dependence in the Δ_k^{I--} state is a direct consequence of the presence of Fermi points instead of FS. We also show the specific heat for the Δ_k^{I--} state in (b), obtained for $V^\Delta = 0.75t_1$ and $\mu = 0$.

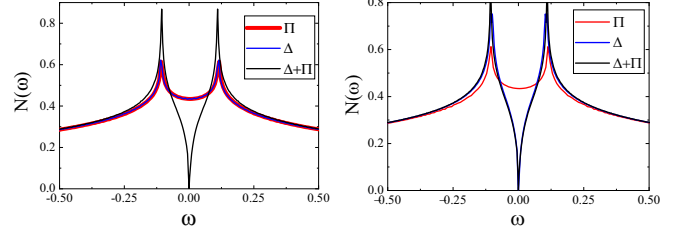


FIG. 7. DOS for $t_2/t_1 = 0$ (left) and $t_2/t_1 = 0.1$ (right) at low T in Δ_k^{I--} (blue), Π_k^{R+-} (red), and the coexistence phase $\Delta + \Pi$ (black). The pairing potentials are $V^\Delta = V^\Pi = 0.75t_1$, and $\mu = 0$.

for finite μ values. Therefore, linear low- T specific heat in the SC state identifies the triplet dPDW state.

The difference in the FS is reflected in the behavior of the electronic density of states $N(\omega)$ accessible by tunneling. In our spinor formalism, $N(\omega) = -\frac{1}{\pi} \text{Im} \sum_{\mathbf{k}} \text{Tr} \{ \mathcal{G}(\mathbf{k}, i\omega_n \rightarrow \omega + i\eta) \}$. Upon performing the analytical continuation, it can be shown to take the form

$$N(\omega) = \sum_{\mathbf{k}} \{ \delta[\omega + E_{\pm}(\mathbf{k})] + \delta[\omega - E_{\pm}(\mathbf{k})] \}. \quad (10)$$

As an example, we present in Fig. 7 the DOS in Π_k^{R+-} , the Δ_k^{I--} state, and the coexistence phase $\Delta + \Pi$ for $t_2/t_1 = 0$ (left) and $t_2/t_1 = 0.1$ (right). For all three states the pairing potentials are $V^\Pi = V^\Delta = 0.75t_1$ for both $t_2/t_1 = 0$ and $t_2/t_1 = 0.1$ and $\mu = 0$.

The vanishing DOS at the Fermi level identifies the coexistence phase $\Delta + \Pi$ in the case of perfect nesting $t_2/t_1 = 0$, whereas for particle-hole asymmetry $t_2/t_1 \neq 0$ the triplet dPDW is the sole state exhibiting a finite DOS at the Fermi level. We stress that the DOS exhibits these characteristic features for both $\mu = 0$ and $\mu \neq 0$. Therefore, tunneling measurements for particle-hole asymmetry may be used to identify the triplet dPDW phase. We note that finite DOS at the Fermi level was also reported in spin-singlet PDW states [18].

IV. Competition of Π_k^{R+-} with $p + ip$

Next, we address the competition of the triplet dPDW state with the $p + ip$ state, which is a widely known stable state in tetragonal systems [28]. In our spinor formalism the $p + ip$ state is written as $\Delta_k^{R--} + \Delta_k^{I--}$, where $\Delta_k^{R--} \sim \sin k_x$ and $\Delta_k^{I--} \sim \sin k_y$. The competition of Π_k^{R+-} with $p + ip$ obeys the following system of coupled gap equations:

$$\begin{aligned} \Delta_{\mathbf{k}}^x &= \sum_{\mathbf{k}'} V_{\mathbf{k},\mathbf{k}'}^x \Delta_{\mathbf{k}'}^x \sum_{\pm} \frac{B_{\mathbf{k}'} \pm \Pi_{\mathbf{k}'}^2}{4E_{\pm}(\mathbf{k}')B_{\mathbf{k}'}} \tanh\left(\frac{E_{\pm}(\mathbf{k}')}{2T}\right), \\ \Delta_{\mathbf{k}}^y &= \sum_{\mathbf{k}'} V_{\mathbf{k},\mathbf{k}'}^y \Delta_{\mathbf{k}'}^y \sum_{\pm} \frac{1}{4E_{\pm}(\mathbf{k}')}} \tanh\left(\frac{E_{\pm}(\mathbf{k}')}{2T}\right), \\ \Pi_{\mathbf{k}} &= \sum_{\mathbf{k}'} V_{\mathbf{k},\mathbf{k}'}^{\Pi} \Pi_{\mathbf{k}'} \sum_{\pm} \frac{B_{\mathbf{k}'} \pm \gamma_{\mathbf{k}'}^2 \pm (\Delta_{\mathbf{k}'}^x)^2}{4E_{\pm}(\mathbf{k}')B_{\mathbf{k}'}} \tanh\left(\frac{E_{\pm}(\mathbf{k}')}{2T}\right), \end{aligned} \quad (11)$$

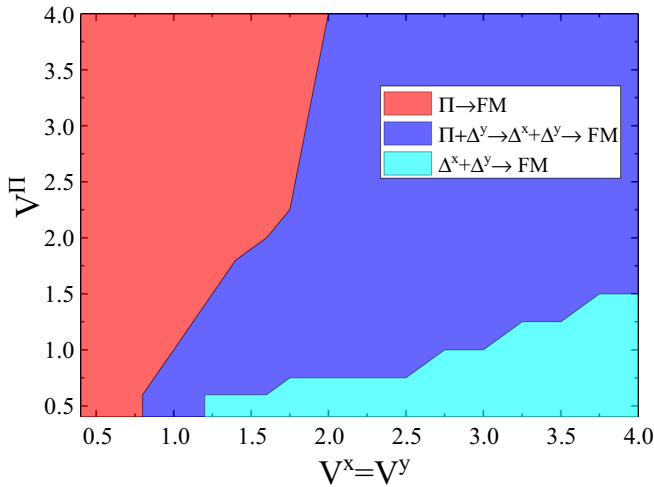


FIG. 8. Maps of the dependence of phase sequences on the effective interactions $V^x = V^y$ and V^Π for low temperature in the case of $\Pi_{\mathbf{k}}^{R+-}$ with $p + ip$. The colors indicate the different cascades of phases obtained when t_2/t_1 grows starting from zero ($\mu = 0$ everywhere). All phases coexist with FM. The phase indicated as FM is only ferromagnetic; no SC gap is finite.

where $B_{\mathbf{k}} \equiv \sqrt{\gamma_{\mathbf{k}}^2[(\delta_{\mathbf{k}} - \mu)^2 + \Pi_{\mathbf{k}}^2] + (\Delta_{\mathbf{k}}^x)^2 \Pi_{\mathbf{k}}^2}$ and the dispersion relations are given by

$$E_{\pm}(\mathbf{k}) = \sqrt{\gamma_{\mathbf{k}}^2 + (\delta_{\mathbf{k}} - \mu)^2 + (\Delta_{\mathbf{k}}^x)^2 + (\Delta_{\mathbf{k}}^y)^2 + \Pi_{\mathbf{k}}^2} \pm 2B_{\mathbf{k}}. \quad (12)$$

The cascades of phases at low temperature as t_2/t_1 grows from zero for various values of the pairing potentials are shown in Fig. 8. Again, the stability of the solutions of the self-consistent equations has been checked by free-energy calculations.

It is remarkable that the triplet dPDW state breaks the stability of the $p + ip$ phase over the largest part of the pairing potential parameter space. Specifically, the formation of the $p + ip$ SC state is disfavored for small deviations from nesting, and a new phase where the triplet dPDW Π^{R+-} state coexists with the y component of $p + ip$, i.e., with Δ^{I--} , is favored at low temperature over a wide range of values of the pairing potentials. This coexistence phase has the following characteristic features. First, the Π gap is always significantly larger, up to one order of magnitude, than the Δ^y gap for particle-hole symmetry. Specifically, for small values of V^y the Δ^y gap is practically zero. As the value of V^y grows, the Δ^y gap grows, but it continues to be much smaller than the Π gap even for $V^y = V^\Pi$. Second, the Δ^y gap remains almost constant as the deviations from nesting grow. The transition from the $\Pi + \Delta^y$ phase to the $p + ip$ state is first order with respect to t_2/t_1 .

An example of the cascade $\Pi + \Delta^y \rightarrow \Delta^x + \Delta^y \rightarrow \text{FM}$ for $V^{x,y} = t_1$, $V^\Pi = 0.75t_1$, and $\mu = 0$ is shown in Fig. 9(a). The Π gap is finite up to $t_2/t_1 \approx 0.11$. The critical temperature for the triplet dPDW state satisfies $T_c/t_1 = 0.045$. In Fig. 9(b) we show the dependence of the gaps on the chemical potential for $t_2/t_1 = 0.1$. We note that the Π gap is maximum for finite μ , while the Δ^y gap practically remains constant as μ grows.

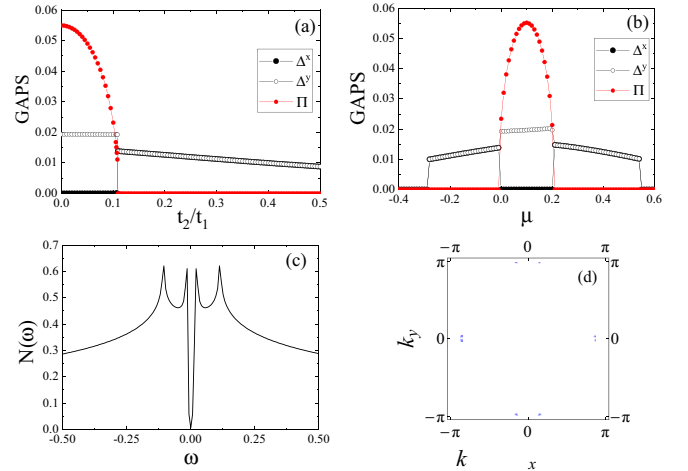


FIG. 9. (a) Dependence of Π , Δ^x , and Δ^y gaps on t_2/t_1 at low T for $\mu = 0$. (b) Dependence of gaps on the chemical potential for $t_2/t_1 = 0.1$. The Π gap is maximum for $\mu = 0.1$. (c) DOS and (d) Fermi surface for $t_2/t_1 = 0.1$. The pairing potentials are $V^x = V^y = t_1$, $V^\Pi = 0.75t_1$.

Again, the Π gap is much larger than the $\Delta^{x,y}$ gaps. Finally, we note that the coexistence phase $\Pi + \Delta^y$ extends to higher t_2/t_1 values for $\mu \neq 0$ at low T , e.g., up to $t_2/t_1 \approx 0.21$ for $\mu = 0.1$.

The $\Pi + \Delta^y$ phase is characterized by a nodal FS for both $t_2 = 0$ and $t_2 \neq 0$, regardless of the value of μ . Thus, the DOS is expected to fall to zero at the Fermi level. An example of this behavior is shown in Fig. 9, where the DOS is presented for $t_2/t_1 = 0.1$. We also note that the specific heat at low temperatures in the $\Pi + \Delta^y$ phase has a polynomial dependence. Therefore, specific heat or tunneling spectroscopy measurements at low temperature identify the pure triplet dPDW state. Finally, we note that if we consider the competition of the $\Pi_{\mathbf{k}}^{I+-}$ state with the $p + ip$ state, the sole change in Fig. 8 is that the coexistence phase is $\Pi + \Delta^x$; that is, the triplet dPDW state coexists with the x component of the $p + ip$. This coexistence phase has the same low-temperature characteristics as the $\Pi + \Delta^x$ phase.

V. SUMMARY AND CONCLUSIONS

In summary, we explored systematically the interplay of all possible triplet SC states in a spinless system within a microscopic mean-field model. We used a tight-binding dispersion that exhibits nesting properties in order to accommodate the presence of commensurate pair density wave SC states. Symmetry allows the existence of two such PDW states. One of them, the triplet PDW state $\Pi_{\mathbf{k}}^{R(I)-+}$, which has p -wave symmetry, can never survive the homogeneous triplet SC states. However, the other triplet PDW $\Pi_{\mathbf{k}}^{R(I)+-}$, with d -wave symmetry, may either appear alone or coexist with the homogeneous SC OPs for small, but finite, deviations from nesting. Specific heat or tunneling measurements at low- T , may be used to identify this state. Our findings are applicable to strongly ferromagnetic systems that develop superconductivity when similar nesting or band structure properties hold.

ACKNOWLEDGMENTS

We are grateful to P. Kotetes for useful discussions.

- [1] S. S. Saxena, P. Agarwal, K. Ahilan, F. M. Grosche, R. K. W. Haselwimmer, M. J. Steiner, E. Pugh, I. R. Walker, S. R. Julian, P. Monthoux, G. G. Lonzarich, A. Huxley, I. Sheikin, D. Braithwaite, and J. Flouquet, *Nature (London)* **406**, 587 (2000).
- [2] D. Aoki, A. Huxley, E. Ressouche, D. Braithwaite, J. Flouquet, J.-P. Brison, E. Lhotel, and C. Paulsen, *Nature (London)* **413**, 613 (2001).
- [3] N. T. Huy, A. Gasparini, D. E. de Nijs, Y. Huang, J. C. P. Klaasse, T. Gortenmulder, A. de Visser, A. Hamann, T. Görlach, and H. v. Löhneysen, *Phys. Rev. Lett.* **99**, 067006 (2007).
- [4] R. S. Keizer, S. T. B. Goennenwein, T. M. Klapwijk, G. Miao, G. Xiao, and A. Gupta, *Nature (London)* **439**, 825 (2006).
- [5] J. Wang, M. Singh, M. Tian, N. Kumar, B. Liu, C. Shi, J. K. Jain, N. Samarth, T. E. Mallouk, and M. H. W. Chan, *Nat. Phys.* **6**, 389 (2010).
- [6] T. S. Khaire, M. A. Khasawneh, W. P. Pratt, and N. O. Birge, *Phys. Rev. Lett.* **104**, 137002 (2010).
- [7] F. S. Bergeret, A. F. Volkov, and K. B. Efetov, *Rev. Mod. Phys.* **77**, 1321 (2005).
- [8] A. I. Buzdin, *Rev. Mod. Phys.* **77**, 935 (2005).
- [9] M. Eschrig, J. Kopu, J. C. Cuevas, and G. Schön, *Phys. Rev. Lett.* **90**, 137003 (2003).
- [10] M. Eschrig, T. Löfwander, T. Champel, J. C. Cuevas, J. Kopu, and G. Schön, *J. Low Temp. Phys.* **147**, 457 (2007).
- [11] A. F. Volkov and K. B. Efetov, *Phys. Rev. Lett.* **102**, 077002 (2009).
- [12] N. Reyren, S. Thiel, A. D. Caviglia, L. Fitting Kourkoutis, G. Hammerl, C. Richter, C. W. Schneider, T. Kopp, A.-S. Rüetschi, D. Jaccard *et al.*, *Science* **317**, 1196 (2007); A. D. Caviglia, S. Gariglio, N. Reyren, D. Jaccard, T. Schneider, M. Gabay, S. Thiel, G. Hammerl, J. Mannhart, and J.-M. Triscone, *Nature (London)* **456**, 624 (2008).
- [13] L. Li, C. Richter, J. Manhart, and R. C. Ashoori, *Nat. Phys.* **7**, 762 (2011).
- [14] K. Michaeli, A. C. Potter, and P. A. Lee, *Phys. Rev. Lett.* **108**, 117003 (2012).
- [15] A. Aperis, G. Varelogiannis, P. B. Littlewood, and B. D. Simons, *J. Phys.: Condens. Matter* **20**, 434235 (2008); A. Aperis, *J. Supercond. Novel Magn.* **22**, 115 (2009); A. Aperis, G. Varelogiannis, and P. B. Littlewood, *Phys. Rev. Lett.* **104**, 216403 (2010).
- [16] Y. Yanase and M. Sigrist, *J. Phys. Soc. Jpn.* **78**, 114715 (2009); D. F. Agterberg, M. Sigrist, and H. Tsunetsugu, *Phys. Rev. Lett.* **102**, 207004 (2009).
- [17] M. Kenzelmann, Th. Strässle, C. Niedermayer, M. Sigrist, B. Padmanabhan, M. Zolliker, A. D. Bianchi, R. Movshovich, E. D. Bauer, J. L. Sarrao, and J. D. Thompson, *Science* **321**, 1652 (2008).
- [18] F. Loder, A. P. Kampf, and T. Kopp, *Phys. Rev. B* **81**, 020511(R) (2010); F. Loder, S. Graser, A. P. Kampf, and T. Kopp, *Phys. Rev. Lett.* **107**, 187001 (2011).
- [19] R. Soto-Garrido and E. Fradkin, *Phys. Rev. B* **89**, 165126 (2014).
- [20] P. A. Lee, *Phys. Rev. X* **4**, 031017 (2014).
- [21] R. Soto-Garrido, G. Y. Cho, and E. Fradkin, *Phys. Rev. B* **91**, 195102 (2015).
- [22] Y. Wang, D. F. Agterberg, and A. Chubukov, *Phys. Rev. B* **91**, 115103 (2015); *Phys. Rev. Lett.* **114**, 197001 (2015).
- [23] K. Seo, H. D. Chen, and J. Hu, *Phys. Rev. B* **78**, 094510 (2008).
- [24] P. Corboz, T. M. Rice, and M. Troyer, *Phys. Rev. Lett.* **113**, 046402 (2014).
- [25] H. D. Chen, O. Vafek, A. Yazdani, and S. C. Zhang, *Phys. Rev. Lett.* **93**, 187002 (2004).
- [26] D. F. Agterberg and H. Tsunetsugu, *Nat. Phys.* **4**, 639 (2008); E. Berg, E. Fradkin, S. A. Kivelson, *ibid.* **5**, 830 (2009); S. Tsonis, P. Kotetes, G. Varelogiannis, and P. B. Littlewood, *J. Phys.: Condens. Matter* **20**, 434234 (2008).
- [27] P. Fulde and R. A. Ferrell, *Phys. Rev.* **135**, A550 (1964); A. I. Larkin and Yu. N. Ovchinnikov, *Sov. Phys. JETP* **20**, 762 (1965).
- [28] C. Kallin and J. Berlinsky, *Rep. Prog. Phys.* **79**, 054502 (2016).